

the SGR estimation algorithm. Section 5 provides an investigation of the SGR estimator's performance, detailing the estimator's advantages, and estimation results. The final section, Conclusions, discusses the results, and provides the final statements of this study.

2. Related work

Many important cultivation process variables, such as SGR and biomass concentrations, cannot be directly measured in real time because biotechnology processes have complex relationships between the processes and variables. The best way to express unmeasurable parameters in real time is to use appropriate soft sensors/estimators [9].

One of the attractive ways to estimate SGR is the direct use of biomass concentration measurements. However, this approach faces difficulties in online measurements of biomass concentration, which is a challenging state variable to measure accurately in a liquid culture [10] noninvasively when various cultivation conditions are to be tested online. This is particularly true for non-stationary processes at the upstream bioprocess development stage. A dielectric spectrometer was used to estimate the biomass concentration and implement an observer-based estimator of the SGR [11]. However, the developed estimation algorithm requires an accurate tuning of the estimator parameters. Moreover, oscillations and instability in estimator performance occur at low biomass concentrations. An SGR estimation approach using biomass concentration measurements obtained through dielectric spectroscopy was presented in [12]. However, the calculated SGR values suffered from biomass measurement uncertainty, which could be reduced by increasing the observation window. However, a large observation window increased the SGR signal delay.

Because online analyzers of biomass concentration are often unavailable or not sufficiently reliable, the SGR needs to be estimated through directly measurable variables, such as the substrate consumption, oxygen uptake rate, carbon dioxide production rate, and base consumption rate [7,10]. For example, the successful implementation of unscented Kalman filters (UKF) combined with an artificial neural network for estimating the SGR based on cumulative oxygen consumption and carbon dioxide production measurements was reported by Simutis and Lübbert [13]. An advanced Kalman filter (EKF) is also suitable for SGR and biomass concentration estimations, where the oxygen uptake rate is one of the input signals [14,15].

Rocha et al. [6] presented a biomass observer that involved the development of an SGR estimator for the fed-batch bioprocess of recombinant *E. coli*, for which online measurements of the dissolved oxygen, oxygen transfer rate, and culture weights were used. The observer and estimator algorithms are based on the asymptotic observer approach, a mathematical model, and the assumption that the model parameters are known. The development of a complex SGR estimation algorithm requires specific knowledge and is a time-consuming task. For example, SGR estimation, data-driven models such as artificial neural networks (ANNs), and hybrid models can be employed, especially in industrial processes. A large amount of data can be used to train and validate ANN-based models [16,17]. However, the ANN and hybrid model approaches entail considerable performance trade-offs and design costs to select proper experimental data and training for ANNs. In addition, each ANN-based estimator applies only to a specific cultivation process. Therefore, the complex approaches that result in complex algorithms are not attractive for developing robust SGR estimators for industrial applications.

In this study, we developed a robust and straightforward estimator of cell biomass SGR in batch and fed-batch cultivation pro-

cesses based on online estimates of the oxygen uptake rate. The algorithm is simple because it requires only two inputs: the OUR and a tuning parameter that uses the stoichiometric parameter ratio. The reliability and simplicity of the SGR estimator make it easy to implement it into the control system as feedback (1).

3. Materials and methods

3.1. Medium and culture conditions

In this work, due to data availability, three types of *Escherichia coli* cell-strain cultivation data were studied to verify the SGR estimates and determine their reliability and versatility. The *E. coli* BL21(DE3) pET9a-IdeS, *E. coli* BL21 (DE3) pET21-IFN- α -5, and *E. coli* BL21(DE3) pLysS were chosen as the study subjects. All three cell strains were cultivated in several independent R&D laboratories.

The cell strain of *E. coli* BL21 (DE3) pET21-IFN- α -5 was cultivated in a 7 L bioreactor. The cultivation medium featured minimal mineral concentrations, including 46.55 g potassium dihydrogen phosphate, 14 g ammonium phosphate dibasic, 5.6 g citric acid monohydrate, 3 ml of concentrated antifoam, 35 g magnesium sulfate heptahydrate, and 105 g D (+) glucose monohydrate. The initial weight of the medium was 3.7 kg. The environmental parameters of the cultivation process remained constant throughout the experiment. The temperature was set to 37 °C, the DOT was set to 20% of air saturation, and the pH was maintained at pH 6.8 through the addition of NaOH(aq). The stirrer speed ranged from 800 to 1200 rpm. The airflow scope ranged from 1.75 to 3.75 L/min. During the cultivation process, pure oxygen flow from 0 to 7.5 L/min was used to increase the oxygen transfer rate in the bioreactor.

E. coli BL21 (DE3) pET9a-IdeS cell strain was cultivated in a 15 L bioreactor. The cultivation medium was introduced according to the minimum requirements of a mineral medium. During the cultivation process, the environmental parameters were as follows: temperature, 37 °C; DOT, 30% of air saturation; and pH maintained at 6.98 via the addition of NaOH(aq). The stirrer speed ranged from 300 to 750 rpm. The operating airflow range ranged from 0.3 to 15 L/min. Pure oxygen flow was provided to the bioreactor during the cultivation process from 0 to 7.5 L/min. During cultivation of the *E. coli* BL21 (DE3) pET21-IFN- α -5 and *E. coli* BL21 (DE3) pET9a-IdeS cell strains. During the *E. coli* BL21 (DE3) pET21-IFN- α -5 and *E. coli* BL21 (DE3) pET9a-IdeS cell cultivation processes, the oxygen concentration in the off-gas from the bioreactor was measured online using a BlueSens BlueInOne Ferm gas analyzer, which had a measuring range from 0 to 100%.

The *E. coli* (BL21(DE3) pLysS) cell strain was cultivated in minimal mineral medium. This medium was composed of (NH₄)₂SO₄,

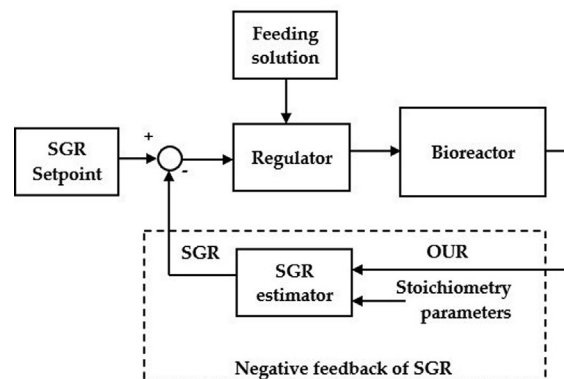


Fig. 1. Principal scheme of the SGR control system.

2.46 g/L; NH4Cl, 0.5 g/L; NaH2PO4 × H2O, 3.6 g/L; Na2SO4, 2 g/L; K2HPO4, 14.6 g/L; (NH4)2-citrate, 1 g/L; 1 M MgSO4 solution, 5 mL/L; trace element solution, 2 mL/L; and no glucose. The initial mass of all cultivations was 5 kg. The pH was kept constant at pH 7, and the temperature was set to 30 °C. DO was set to 30% saturation. The bioreactor had a working volume of 15 L (Biostat C, Sartorius Stedim Biotech), and the stirrer speed varied from 100 to 1400 rpm. The oxygen uptake rate, OUR, was measured online with a paramagnetic oxygen sensor placed in the reactor's vent line behind the offgas cooler (Sidor, Sick-Maihak, Hamburg).

4. Development of the SGR estimation algorithm

Cells are living organisms that breathe and consume food (glucose), so respiratory data can express the state of the cell culture in the bioreactor. The higher the biomass content, the more evident is the respiration data. The main parameters of respiratory data are the oxygen uptake rate (OUR) and carbon dioxide production rate (CPR). In this study, the algorithm for the online estimation of SGR during microbial cultivation processes relies upon reasonable estimates of the OUR, as the OUR signal is less sensitive to cellular metabolism and other negative cell growth phenomena than the CPR signal. The oxygen uptake rate can be calculated online from the difference between the oxygen concentration entering the bioreactor and the oxygen concentration leaving the bioreactor [18,19]:

$$OUR(t) = Q \cdot (O_2^{in} - O_2^{out}); \tag{1}$$

where O_2^{in} and O_2^{out} are the oxygen concentrations at the inlet and outlet gas streams, and Q is the gas flow rate. The relationship between the OUR and biomass growth in microbial cultures can be modeled using Luedeking/Piret-type relationships [20,21]:

$$OUR(t) = \alpha \cdot X(t) + \beta \cdot X(t); \tag{2}$$

$$\frac{dX}{dt} = \mu \cdot X(t), \tag{3}$$

where X is the amount of cell biomass in the bioreactor, μ is the SGR, t is time, and α and β are stoichiometry parameters.

The stoichiometric coefficients α and β define the cell metabolism of oxygen consumption. Stoichiometry means that the same cell strain has the same coefficients or forms. In Eq. (2), the coefficient α describes a specific cell's oxygen consumption yield ($\alpha \equiv Y_{O_2/X}$) for growth, while β is a coefficient representing the oxygen consumption for maintenance ($\beta \equiv m_{O_2/X}$) [22,23,7].

Taking the derivative of Eq. (2) with respect to time and combining it with Eq. (3), we obtain:

$$\frac{dOUR(t)}{dt} = \alpha \cdot \frac{d\mu}{dt} \cdot X(t) + OUR(t) \cdot \mu. \tag{4}$$

Eq. (4) can then be reconstructed to eliminate the biomass parameter X to make the algorithm dependent only on OUR and stoichiometry:

$$\frac{1}{OUR(t)} \cdot \frac{dOUR(t)}{dt} = \frac{1}{\mu + \beta/\alpha} \cdot \frac{d\mu}{dt} + \mu. \tag{5}$$

Parameter R denotes the dynamics of oxygen consumption:

$$R = \frac{1}{OUR(t)} \cdot \frac{dOUR(t)}{dt}. \tag{6}$$

The differential equation can then be used to represent the dynamic relationship between the SGR values μ and R :

$$\frac{1}{\mu + \beta/\alpha} \cdot \frac{d\mu}{dt} + \mu = R. \tag{7}$$

One can also use the first-order transfer function:

$$G_{\mu/R}(s) = \frac{1}{Ts + 1}, \tag{8}$$

where s is the Laplace variable, and T is the time constant related to the SGR.

$$T = \frac{1}{\mu + \beta/\alpha}. \tag{9}$$

The dynamic relationship between OUR and R is defined by the differentiator transfer function

$$G_{R/OUR}(s) = ks, \tag{10}$$

where $k = 1/OUR$. The resulting transfer function relating the OUR to the SGR is as follows:

$$G_{\mu/OUR}(s) = \frac{ks}{Ts + 1}. \tag{11}$$

The discrete OUR measurement-based SGR estimation algorithm is then obtained from the transfer function (11) by applying the z -transform. The discrete algorithm of the SGR estimator is illustrated in Fig. 2.

In the structure scheme of the SGR estimator (Fig. 2), the first part is intended for calculating the parameter R_n , which conveys the dynamics of oxygen consumption:

$$R_n = OUR_n \cdot \frac{k(1 - z^{-1})}{\Delta t}. \tag{12}$$

By applying the z -transform for Eq. (12), where $k = 1/OUR_n$, the results yield

$$R_n = \frac{1}{OUR_n} \cdot \frac{OUR_n - OUR_{n-1}}{\Delta t}. \tag{13}$$

The last part of the structure diagram of the SGR estimator shows the relationship between the dynamics of oxygen consumption and the time constant, which gives the value of the SGR:

$$\mu_n = R_n \cdot \frac{\Delta t}{T(1 - z^{-1}) + \Delta t}. \tag{14}$$

The final formula for the SGR estimator is obtained by applying the z -transform to Eq. (14):

$$\mu_n = R_n \cdot \frac{\Delta t}{T + \Delta t} + \mu_{n-1} \cdot \frac{T}{T + \Delta t}, \tag{15}$$

where $T = 1/(\mu_{n-1} + (\beta/\alpha))$.

The presented SGR estimator is versatile and can be applied to the monitoring of various cultivation processes. A single turning parameter is the stoichiometric parameter ratio β/α , which is specific to a particular strain of microorganisms and can be found in reference books or estimated from early batch culture experiments [24]. For many cell strains and in many cultivation processes, the maintenance term β is negligible. The ratio β/α (typically 0.01–0.04) is usually smaller than the SGR by orders of magnitude. Therefore, even using a zero value for β/α in the estimation algorithm provides interpretable SGR estimation results.

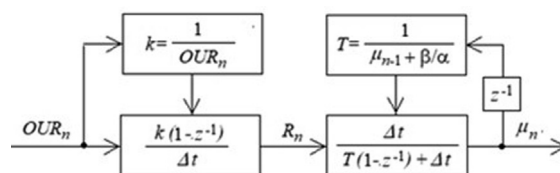


Fig. 2. Block scheme of the SGR estimation algorithm (z^{-1} is the backward-shift operator, Δt is the sampling time, and n is the number time discretization point).

5. Investigation of the SGR estimator performance

5.1. Computer simulation

The first step in assessing the performance of the SGR estimator was chosen by computer simulation using the MATLAB/Simulink platform. In the simulation, different fed-batch cultivation processes with different SGR time profiles were modeled by varying the feeding speed of the feeding solution. A mathematical model of the *E. coli* cultivation process is described in [25,26]. The following differential equation describes the biomass concentration (g/L):

$$\frac{dx}{dt} = \mu(s) \cdot x - F \cdot \frac{x}{V}, \quad (16)$$

where x is the biomass concentration, g/L; μ is the specific biomass growth rate (1/h); V is the volume of the liquid culture, L; F is the substrate feeding rate, g/h; and t is the process time, h. Another differential equation describing the glucose concentration in a bioreactor (in g/L) is as follows:

$$\frac{ds}{dt} = -q_s(s) \cdot x + F \cdot \frac{s_f - s}{V}, \quad (17)$$

where q_s is the specific substrate consumption rate, g/(g·h), and s_f is the substrate concentration in the feeding solution (g/L). The volume of the medium in the bioreactor depends directly on the feeding speed of the feeding solution.

$$\frac{dV}{dt} = F. \quad (18)$$

The oxygen uptake rate signal is calculated using the Luedeking/Piret model (g/(h·V)):

$$OUR = \alpha \cdot \mu(s) \cdot x \cdot V + \beta \cdot x \cdot V. \quad (19)$$

The dependence of the relative growth rate on the substrate concentration can be mathematically expressed using the Monod model [27,28]:

$$\mu(s) = \mu_{max} \cdot \frac{s}{k_s + s} \cdot \frac{k_i}{k_i + s}, \quad (20)$$

where μ_{max} is the maximum possible specific growth rate of the specific cell culture, and k_s and k_i are the Monod expression parameters indicating the inhibition of the cell culture by overfeeding. Finally, the simulation's mathematical expression describing the relative substrate consumption rate (in g/(g·h)) is as follows:

$$q_s(s) = \frac{\mu(s)}{Y_{x/s}} + m, \quad (21)$$

where $Y_{x/s}$ is a specific cell culture yield factor that describes the need for a certain amount of food (glucose) for a certain amount of biomass (g/g), and m refers to the model parameters that define the food requirements for biomass maintenance, g/(g·h).

The parameters of the model Eqs. (12)–(17) and the initial values of the state variables in the simulation experiments are listed in Table 1.

In the simulation experiments, various time profiles of the SGR were obtained by manipulating the feed rate. Feed-rate interruption disturbances were also added to the feed-rate time profiles to simulate the complicated process control conditions. As the actual measurements of the OUR are usually corrupted by noise, the measurements applied in the recursive estimation algorithm (Fig. 2) were simulated by adding white Gaussian noise:

$$OURm_n = OUR_n + \sigma \cdot OUR_n \cdot Rand, \quad (22)$$

where $OURm$ is the measured value of OUR; the percentage standard deviation of the absolute OUR value estimated from observations is σ ($\sigma = 3\%$), $Rand$ is a number from the Gaussian random

Table 1
Values of model parameters.

Parameter	Value	Dimension
k_i	85	g/L
k_s	0.7	g/L
m	0.02	g/(g·h)
s_f	150	g/L
$Y_{x/s}$	0.8	g/g
α	0.82	g/g
β	0.01	g/(g·h)
μ_{max}	1.1	1/h
$x(0)$	0.5	g/L
$s(0)$	5.0	g/L
$V(0)$	8.0	L

number sequence with zero mean and unit variance, and subscript n denotes the count of discrete measurement points.

In the simulation experiments, the time discretization step of the recursive estimation algorithm was set to $\Delta t = 0.0025$ h, and the ratio β/α (tuning parameter) value was determined to be $\beta/\alpha = 0.01$.

Preliminary simulation experiments showed problems in the estimator's performance during the initial stage of the cultivation process. The convergence rate to the actual value of SGR at the beginning of the process was sensitive to the initial value of the SGR entered into the recursive algorithm (Fig. 2). The OUR estimation errors significantly corrupted the estimator's performance in the initial stage of the cultivation process when the OUR signal-to-noise ratio was low [6]. It was discovered that the initial measurement-based estimate of the variable (Eq. 7 provides a valid first-approach value for the SGR in the recursive estimation algorithm. Therefore, the initial SGR value can also be estimated from the early cultivation experiments. The above estimator performance problems can be resolved by switching the estimator output after some time once the OUR increases, and the estimation algorithm captures the actual value of the SGR. A proper time point for enabling the estimator was found to be 1–3 h into the cultivation process in the simulation platform.

The results of the simulation experiments under various cultivation conditions are presented in Fig. 3 (Experiments I and II). The time trajectories of the feeding rate applied to simulate different cultivation conditions are shown in Fig. 3a. The trajectories of biomass growth are shown in Fig. 3b. The simulated values of the OUR measurements $OURm_n$, upon which the SGR estimation is based, are shown in Fig. 3c. The estimator's performance in tracking time-varying biomass SGR is illustrated in Fig. 3d, in which the estimated SGR trajectories (solid lines) are compared with the actual trajectories (dotted lines).

The simulation results presented in Fig. 3 (Experiments I and II) show that the proposed estimator offers accurate SGR estimates during fed-batch cultivation processes under feeding rate disturbances and OUR measurement noise.

5.2. Experimental testing

The SGR estimator's performance and reliability were investigated using actual *E. coli* cultivation process data. Experimental SGR values and OUR data for the oxygen uptake rate were collected from fed-batch experiments of *Escherichia coli* obtained from [29] and industrial R&D laboratories. To cover more practical scenarios, three types of *E. coli* cell strains were used in different sizes of bioreactors:

1. The *E. coli* BL21 (DE3) pET21-IFN-alfa-5 cell strain was cultivated in a 7 L bioreactor. Eleven fed-batch cultivations were performed, where eight cultivations were carried out with a growth-limiting feed rate and three without a growth-limiting feed rate, that is, batch or repetitive batch processes.

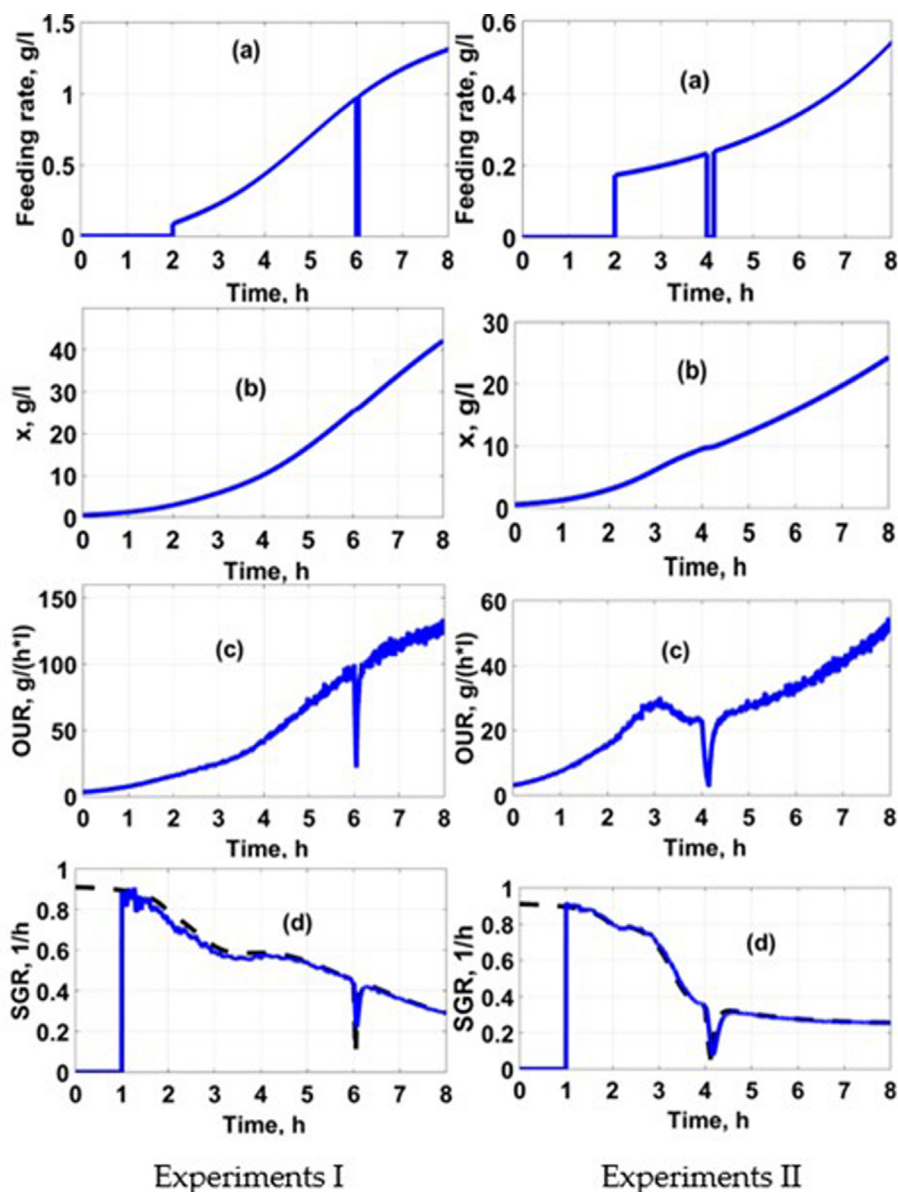


Fig. 3. Simulation results of the SGR estimator performance by tracking various SGR time trajectories (Experiments I, II): (a), (b), (c) feeding rate, biomass growth, and oxygen uptake rate curves, respectively; d) comparison of the simulated SGR versus estimated SGR curves (dotted and solid lines, respectively).

2. The *E. coli* BL21 (DE3) pET9a-IdeS cell strain was cultivated in a 12 L bioreactor. Two cultivations were performed at a growth-limiting rate.
3. The *E. coli* (BL21(DE3) pLysS) cell strain was cultivated in a 15 L bioreactor. Seven fed-batch cultivations under growth-limiting rate conditions were selected for SGR estimator inspection.

The offline biomass concentration values in the cultivation experiments were determined from the measurements of the optical density OD (in o.u.) multiplied by the coefficient of the biomass concentration (approximately 0.4 g/L/o.u.) [30]. The experimental SGR values were calculated from offline biomass concentration values collected from the sample measurements. The stoichiometry parameters of cell cultures α and β were determined using the literature and experimental data [24]. In this work, the values for the stoichiometry parameters of oxygen consumption remained the same in all *E. coli* cell cultures (ratio $\beta/\alpha = 0.04$).

The precision and reliability of the SGR estimator were evaluated by comparing the estimator predictions with the SGR values calculated offline from the biomass growth curve approximating the biomass concentration measurements. To describe the SGR estimator results, the indicators of mean absolute error (MAE) and root mean square error (RMSE) were applied. The MAE method evaluates the errors between the estimated and observed biomass values during the cultivation process. The MAE approach is defined as follows [31]:

$$MAE = \frac{\sum_{i=1}^n |\hat{y}_i - y_i|}{n}, \quad (23)$$

where n is the number of data counts, and \hat{y}_i is the estimation result compared to y_i , which is the value determined through the cultivation process. The root mean square error represents the square root

of the residuals of the differences between the predicted and observed values. The RMSE formula is as follows [31]:

$$RMSE = \sqrt{\frac{\sum_{i=1}^n (\hat{y}_i - y_i)^2}{n}} \tag{24}$$

The SGR estimator results for the three different cell strains are shown below.

Three experiments (9–11) were performed with a dose-unlimited substrate feeding. The rest of the experiments were provided limited feeding using the various control strategies described in [32], with multiple substrate-limited feeding profiles. The

Table 2
Analysis of *E. coli* BL21 (DE3) pET21-IFN-alfa-5, 7 L bioreactor.

Exp. No.	RMSE, 1/h	MAE, 1/h
1	0.034	0.027
2	0.054	0.047
3	0.056	0.040
4	0.051	0.036
5	0.050	0.038
6	0.045	0.038
7	0.054	0.046
8	0.057	0.040
9	0.040	0.035
10	0.041	0.030
11	0.034	0.030

Table 3
Analysis of *E. coli*(BL21(DE3) pLysS), 15 L bioreactor.

Exp. No.	RMSE, 1/h	MAE, 1/h
1	0.058	0.054
2	0.056	0.048
3	0.049	0.036
4	0.058	0.053
5	0.050	0.042
6	0.062	0.048
7	0.059	0.048

Table 4
Analysis of *E. coli*(BL21(DE3) pET9a-IdeS), 12 L bioreactor.

Exp. No.	RMSE, 1/h	MAE, 1/h
1	0.060	0.050
2	0.053	0.044

human factors and equipment influenced the results, as shown in Tables 2–4. Because the samples were taken manually, the SGR experimental values featured errors that affected the outcomes of the estimates. The overall average MAE of the SGR was 0.042 1/h, and the overall average RMSE of the SGR estimation was 0.051 1/h. These results show that this approach is acceptable for both limited and unlimited fed-batch cultivation processes with various *E. coli* cell strains.

At the beginning of the cultivation process, the SGR estimator requires an initial SGR value. This can be done in two ways to obtain an initial SGR value. The first method uses two biomass concentration values taken from the measurement samples at the beginning of the cultivation process and calculate the initial SGR value. This method allows the use of the SGR estimator at the beginning of the cultivation process when two samples are taken at an interval of at least half an hour. This method is suitable if data monitoring does not start from the beginning of inoculation and when offline OD values are available. The second method (recommended by the authors of this study) uses the initial value of the SGR value set to zero. This method can be used when data monitoring of the cultivation process data started immediately after the inoculation or when the cells were still dormant. At the inoculation moment, the cells have the stress of a new environment and must be prepared for reproduction. This phase is called the lag phase. The cells prepare ferments to start reproduction; hence, in the lag phase, the specific growth rate is equal to zero [33,34]. This method allows the use of the SGR estimator at the beginning of the cultivation process after inoculation without any measurements of the biomass. As shown in Figs. 4–6, the SGR estimator begins to run the start of the cultivation process.

During online monitoring of the cultivation experiments, the SGR estimator demonstrated robust behavior and consistency between the SGR online estimates and the rough SGR observations obtained from the discrete offline biomass concentration measurements.

6. Conclusions

In this study, an estimator of the biomass-specific growth rate was developed for online monitoring of microbial cultivation processes. The estimation algorithm is based on a functional model and measurements of the oxygen uptake rate.

The computer simulation of our specific-growth-rate estimator revealed robust behavior of the recursive estimation algorithm and sufficiently accurate tracking of the specific-growth-rate time trajectories under process disturbances and measurement errors of

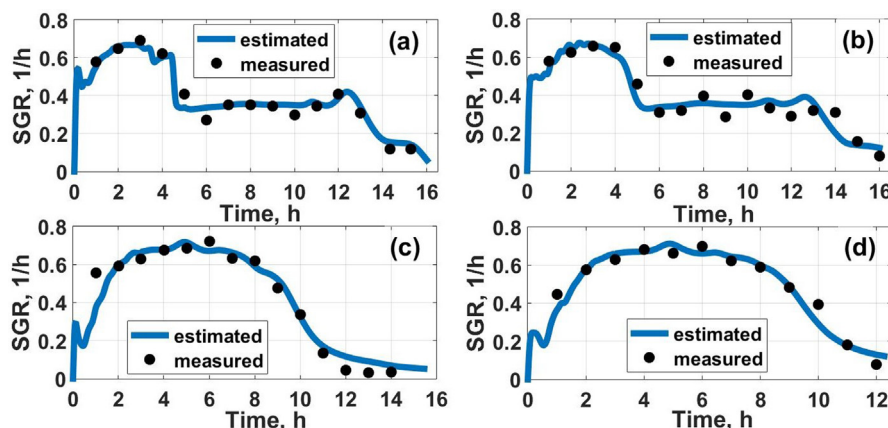


Fig. 4. SGR estimation results with cultivation process data: a) Exp. 1 Table 2, limited fed-batch cultivation processes; b) Exp. 2 Table 2, limited fed-batch cultivation process; and c) Exp. 9 Table 2, unlimited fed-batch cultivation process; d) Exp. 10 Table 2 and the unlimited fed-batch cultivation process.

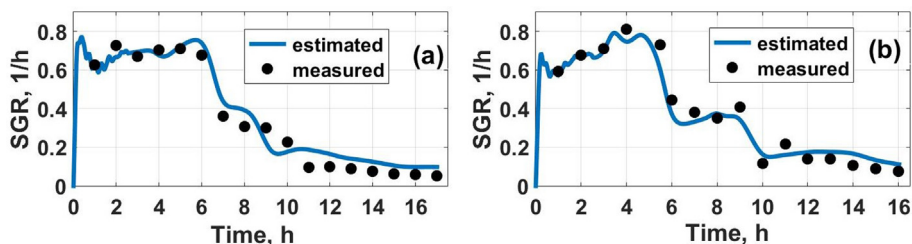


Fig. 5. SGR estimation results with limited feeding solution fed-batch cultivation process data: a) Exp. 1 Table 3; b) Exp. 2 Table 3.

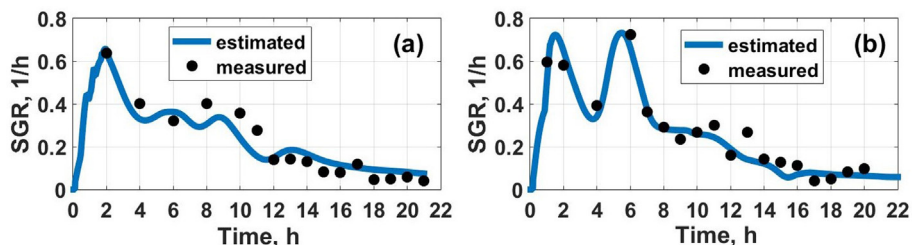


Fig. 6. SGR estimation results with limited feeding solution fed-batch cultivation process data: a) Exp. 1 Table 4; b) Exp. 2 Table 4.

the off-gas parameters. The experimental investigation estimator was established using three different *E. coli* strains in bioreactors with several different working volumes. The overall average MAE of the SGR was 0.044 1/h, and the overall average RMSE of the SGR estimation was 0.074 1/h.

This estimator can be applied to the online monitoring of various cultivation processes with limited or unlimited substrate feeding. This method requires adjusting only a single tuning parameter, that is, the ratio of β/α , to adapt the estimator to a particular process. An approximate or zero value of the tuning parameter provided satisfactory estimation results. Thus, the presented estimator can provide a proper feedback signal for advanced SGR automatic control systems.

Funding

This project was funded by the European Regional Development Fund (project No 01.2.2-LMT-K-718-03-0039) under a grant agreement with the Research Council of Lithuania (LMTLT).

CRediT authorship contribution statement

Arnas Survyla: Methodology, Software, Validation, Data curation, Writing – original draft, Visualization. **Donatas Levisauskas:** Conceptualization, Methodology, Validation, Formal analysis, Investigation, Writing – original draft. **Renaldas Urniezius:** Methodology, Software, Validation, Resources, Writing – original draft, Writing – review & editing, Supervision. **Rimvydas Simutis:** Formal analysis, Data curation.

Declaration of Competing Interest

The authors declare that they have no known competing financial interests or personal relationships that could have appeared to influence the work reported in this paper.

References

- Tripathi NK, Shrivastava A. Recent developments in bioprocessing of recombinant proteins: expression hosts and process development. *Front Bioeng Biotechnol* 2019;7:420. <https://doi.org/10.3389/fbioe.2019.00420>.
- Schaepe S, Kuprijanov A, Sieblst C, Jenzsch M, Simutis R, Lübbert A. Current advances in tools improving bioreactor performance. *Curr Biotechnol* 2013;3(2):133–44. <https://doi.org/10.2174/2211550102666131217235246>.
- Guidance for Industry PAT – A Framework for Innovative Pharmaceutical Development, manufacturing, and Quality Assurance 19. URL: <https://www.fda.gov/media/71012/download>.
- Urniesius R, Survyla A. Identification of functional bioprocess model for recombinant *E. coli* cultivation process. *Entropy* 2019;21(12):1221. <https://doi.org/10.3390/e21121221>. URL: <https://www.mdpi.com/1099-4300/21/12/1221>.
- Urniesius R, Kemesis B, Simutis R. Bridging offline functional model carrying aging-specific growth rate information and recombinant protein expression: entropic extension of akaike information criterion. *Entropy* 2021;23(8):1057. <https://doi.org/10.3390/e23081057>. URL: <https://www.mdpi.com/1099-4300/23/8/1057>.
- Rocha I, Veloso A, Carneiro S, Costa R, Ferreira E. Implementation of a specific rate controller in a fed-batch *E. coli* fermentation. *IFAC Proc Vol* 2008;41(2):15565–70. <https://doi.org/10.3182/20080706-5-kr-1001.02632>.
- Gnoth S, Jenzsch M, Simutis R, Lübbert A. Control of cultivation processes for recombinant protein production: a review. *Bioprocess Biosyst Eng* 2007;31(1):21–39. <https://doi.org/10.1007/s00449-007-0163-7>.
- Galvanuskas Simutis, Urniezius Levisauskas. Practical solutions for specific growth rate control systems in industrial bioreactors. *Processes* 2019;7(10):693. <https://doi.org/10.3390/pr7100693>.
- Goodwin GC. Predicting the performance of soft sensors as a route to low cost automation. *Annu Rev Control* 2000;24:55–66. [https://doi.org/10.1016/s1367-5788\(00\)90013-0](https://doi.org/10.1016/s1367-5788(00)90013-0).
- Schuler MM, Marison IW. Real-time monitoring and control of microbial bioprocesses with focus on the specific growth rate: current state and perspectives. *Appl Microbiol Biotechnol* 2012;94(6):1469–82. <https://doi.org/10.1007/s00253-012-4095-z>.
- Claes JE, Impe JFV. On-line estimation of the specific growth rate based on viable biomass measurements: experimental validation. *Bioprocess Eng* 1999;21(5):389. <https://doi.org/10.1007/s004490050692>.
- Brignoli Y, Freeland B, Cunningham D, Dabros M. Control of specific growth rate in fed-batch bioprocesses: novel controller design for improved noise management. *Processes* 2020;8(6):679. <https://doi.org/10.3390/pr8060679>.
- Simutis R, Lübbert A. Exploratory analysis of bioprocesses using artificial neural network-based methods. *Biotechnol Prog* 1997;13(4):479–87. <https://doi.org/10.1021/bp9700364>.
- Soons ZITA, van Straten G, van der Pol LA, van Boxtel AJB. Online automatic tuning and control for fed-batch cultivation. *Bioprocess Biosyst Eng* 2007;31(5):453–67. <https://doi.org/10.1007/s00449-007-0182-4>.
- Simutis R, Lübbert A. Bioreactor control improves bioprocess performance. *Biotechnol J* 2015;10(8):1115–30. [https://doi.org/10.1002/1522-2675\(201510\)10:8<1115::aid-biot201500016>3.0.co;2-1](https://doi.org/10.1002/1522-2675(201510)10:8<1115::aid-biot201500016>3.0.co;2-1).
- Desai KM, Vaidya BK, Singhal RS, Bhagwat SS. Use of an artificial neural network in modeling yeast biomass and yield of β glucan. *Process Biochem* 2005;40(5):1617–26. <https://doi.org/10.1016/j.procbio.2004.06.015>.
- Aehle M, Simutis R, Lübbert A. Comparison of viable cell concentration estimation methods for a mammalian cell cultivation process. *Cytotechnology* 2010;62(5):413–22. <https://doi.org/10.1007/s10616-010-9291-z>.
- Garcia-Ochoa F, Gomez E, Santos VE, Merchuk JC. Oxygen uptake rate in microbial processes: an overview. *Biochem Eng J* 2010;49:289–307. <https://doi.org/10.1016/j.bej.2010.01.011>.

- [19] Pappenreiter M, Sissolak B, Sommeregger W, Striedner G. Oxygen uptake rate soft-sensing via dynamic k_{la} computation: cell volume and metabolic transition prediction in mammalian bioprocesses. *Front Bioeng Biotechnol* 2019;7:195. <https://doi.org/10.3389/fbioe.2019.00195>.
- [20] Luedeking R, Piret EL. Transient and steady states in continuous fermentation. theory and experiment. *J Biochem Microbiol Technol Eng* 1959;1(4):431–59. <https://doi.org/10.1002/jbmte.390010408>.
- [21] Luedeking R, Piret EL. A kinetic study of the lactic acid fermentation. batch process at controlled pH. *J Biochem Microbiol Technol Eng* 1959;1(4):393–412. <https://doi.org/10.1002/jbmte.390010406>.
- [22] Unrean P. Bioprocess modelling for the design and optimization of lignocellulosic biomass fermentation. *Bioresour Bioprocess* 2016;3(1). <https://doi.org/10.1186/s40643-015-0079-z>.
- [23] Caramihai M, Severi I. Bioprocess modeling and control. In: *Biomass Now – Sustainable Growth and Use*; InTech; 2013. doi:10.5772/55362..
- [24] Urniezius R, Survyla A, Paulauskas D, Bumelis VA, Galvanauskas V. Generic estimator of biomass concentration for *Escherichia coli* and *Saccharomyces cerevisiae* fed-batch cultures based on cumulative oxygen consumption rate. *Microbial Cell Factories* 2019;18(1). <https://doi.org/10.1186/s12934-019-1241-7>.
- [25] Levisauskas D. *Biotechnol Lett* 2001;23(15):1189–95. <https://doi.org/10.1023/a:1010528915228>.
- [26] Brion K. *Measurement and control in bioprocessing*. London New York: Elsevier Applied Science; 1991.
- [27] Kovárová-Kovar K, Egli T. Growth kinetics of suspended microbial cells: From single-substrate-controlled growth to mixed-substrate kinetics. *Microbiol Mol Biol Rev* 1998;62(3):646–66. <https://doi.org/10.1128/mmb.62.3.646-666.1998>.
- [28] Monod J. The growth of bacterial cultures. *Annu Rev Microbiol* 1949;3(1):371–94. <https://doi.org/10.1146/annurev.mi.03.100149.002103>.
- [29] Schaepe S, Kuprijanov A, Simutis R, Lübbert A. Avoiding overfeeding in high cell density fed-batch cultures of *E. coli* during the production of heterologous proteins. *J Biotechnol* 2014;192:146–53. <https://doi.org/10.1016/j.jbiotec.2014.09.002>.
- [30] Shiloach J, Fass R. Growing *E. coli* to high cell density—a historical perspective on method development. *Biotechnol Adv* 2005;23(5):345–57. <https://doi.org/10.1016/j.biotechadv.2005.04.004>.
- [31] Willmott C, Matsuura K. Advantages of the mean absolute error (MAE) over the root mean square error (RMSE) in assessing average model performance. *Clim Res* 2005;30:79–82. <https://doi.org/10.3354/cr030079>.
- [32] Urniezius R, Galvanauskas V, Survyla A, Simutis R, Levisauskas D. From physics to bioengineering: microbial cultivation process design and feeding rate control based on relative entropy using nuisance time. *Entropy* 2018;20(10):779. <https://doi.org/10.3390/e20100779>.
- [33] Rolfe MD, Rice CJ, Lucchini S, Pin C, Thompson A, Cameron ADS, Alston M, Stringer MF, Betts RP, Baranyi J, Peck MW, Hinton JCD. Lag phase is a distinct growth phase that prepares bacteria for exponential growth and involves transient metal accumulation. *J Bacteriol* 2012;194:686–701. <https://doi.org/10.1128/JB.06112-11>.
- [34] Madar D, Dekel E, Bren A, Zimmer A, Porat Z, Alon U. Promoter activity dynamics in the lag phase of *Escherichia coli*. *BMC Syst Biol* 2013;7:136. <https://doi.org/10.1186/1752-0509-7-136>.